

## Vibrational Spectroscopy of Mechanically Compressed Monolayers

Otto Berg\* and David Klenerman

Contribution from the Department of Chemistry, University of Cambridge, Lensfield Road, Cambridge CB2 1EW, United Kingdom

Received May 31, 2002; Revised Manuscript Received January 31, 2003; E-mail: oberg@wsu.edu

**Abstract:** Sum-frequency spectroscopy has been used to investigate the behavior of self-assembled monolayers in a solid–solid contact. Various alkanethiol layers on gold were observed before, during, and after compression to 660 MPa against a sapphire counterface. Well-ordered layers that differ only in the length of their alkane tails ( $C_8$  versus  $C_{18}$ ) behave similarly. In contrast, defective and partly melted monolayers are more sensitive to stress than are their well-ordered analogues, and they are more prone to irreversible changes. In all cases, the intensity of methyl C–H stretching modes decreases with applied pressure, indicating a loss of net orientational order among the terminal methyl groups. The magnitude of this effect in well-ordered layers can be compared with the theoretical sensitivity of the resonant sum-frequency signal to molecular orientation. On these grounds, an increased population of terminal gauche conformers is identified as the disordering mechanism under pressure.

### Introduction

Mechanical contact between solid objects is mediated by the terminal atoms on each surface. Consequently, contact behavior can be modified by chemical passivation or the presence of an intervening molecular layer. This phenomenon was labeled “boundary lubrication” by W. B. Hardy in 1920, when he reported that a fatty acid monolayer can lower the coefficient of solid/solid sliding friction by an order of magnitude.<sup>1</sup> Subsequent research indicated that the mechanical effects of a boundary lubricant are strongly related to its state of intermolecular order.<sup>2</sup> Despite the technological importance of these effects, an understanding at the chemical level has been slow to develop. Recent progress in bridging the macroscopic and molecular behavior has occurred on two fronts. Experimentally, the atomic force microscope (AFM) and its variants have led to “nanotribology”, the study of frictional forces with atomic resolution.<sup>3</sup> Meanwhile, computational simulations of films under pressure and shear have illustrated how external forces can cause conformational changes.<sup>4,5</sup> It remains a challenge to observe the molecular-level effects in real contacts. Such details will be reflected in the internal states of the molecules involved, which can be probed spectroscopically.

In a material that lacks inversion symmetry, the polarization produced by an incident electromagnetic field of frequency  $\nu$  will differ in magnitude over the two halves of an optical cycle. This adds a frequency component at  $2\nu$  to the scattered light – a form of harmonic distortion that is not possible (in

the electric dipole approximation) for materials that do have inversion symmetry. At the interface between different centrosymmetric solids, for example, this anharmonic optical susceptibility can “add” two photons, although the bulk materials cannot. The polarization anisotropy of second harmonic generation (SHG) has already been used to document orientational changes in a monolayer subjected to mechanical shear.<sup>6</sup> If one of the driving fields is tuned through the infrared, resonant enhancement of the sum-frequency generation (SFG) intensity yields a kind of vibrational spectrum.<sup>7</sup> This carries information about the molecular species present, their orientation, intermolecular coupling, and order. In addition to being intrinsically interface-specific, sum-frequency spectroscopy has submonolayer sensitivity and the ability to access very small contacts. The first published report of SHG and SFG from monolayers in a solid–solid contact found a large reduction in their collective nonlinear optical response.<sup>8</sup> This loss of SFG signal was confirmed in a subsequent study of compressed Langmuir–Blodgett films; at 60 MPa, the resonant SFG had weakened by a factor of 300, while Raman spectra were unaffected.<sup>9</sup> Because the SFG method is sensitive to intermolecular order, both of these studies concluded that contact pressure rearranges an adsorbed layer’s intermolecular structure.

We have recently published SFG spectra from a prototypical self-assembled monolayer, octadecanethiol (ODT) on gold, in contact with a sapphire flat.<sup>10</sup> Again, the intensity of resonant signals decreased under pressure, but this system was much less

(1) Sir William Bate Hardy *Collected Papers*; Cambridge University Press: New York, 1936.  
(2) Bowden, F. P.; Tabor, D. *The Friction and Lubrication of Solids*; Clarendon Press: Oxford, 1950.  
(3) Persson, B. N. J. *Sliding Friction*; Springer: New York, 1998.  
(4) Mikulski, P. T.; Harrison, J. A. *J. Am. Chem. Soc.* **2001**, *123*, 6873–6881.  
(5) Tutein, A. B.; Stuart, S. J.; Harrison, J. A. *Langmuir* **2000**, *16*, 291–296.

(6) Eisert, F.; Gurka, M.; Legant, A.; Buck, M.; Grunze, M. *Science* **2000**, *287*, 468–470.  
(7) Bain, C. D. *J. Chem. Soc., Faraday Trans.* **1995**, *91*, 1281–1296.  
(8) Du, Q.; Xiao, X.-d.; Charych, D.; Wolf, F.; Frantz, P.; Shen, Y. R.; Salmeron, M. *Phys. Rev. B* **1995**, *51*, 7456–7463.  
(9) Beattie, D. A.; Haydock, S.; Bain, C. D. *Vib. Spectrosc.* **2000**, *24*, 109–123.  
(10) Berg, O.; Klenerman, D. *J. Appl. Phys.* **2001**, *90*, 5070–5074.

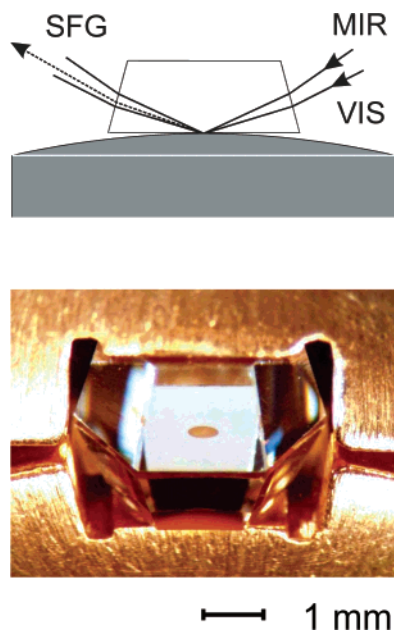


**Figure 1.** Schematic cross-sectional diagram of the pressure cell, and photograph of the contact along the optic axis. The spherical surface is a gold-coated bronze ball with a 25 mm radius of curvature. The flat surface is a synthetic sapphire prism. These are forced together with a pneumatic piston, forming a round area of contact visible against total internal reflection from the prism face. An applied force of 95 N, as here, produces a contact 550  $\mu\text{m}$  in diameter, with a central pressure of 660 MPa. Also shown are the paths of the visible (VIS), mid-infrared (MIR), and sum-frequency beams (SFG).

sensitive. At a stress approaching the strength of the metallic substrate (660 MPa), vibrationally resonant signals had weakened by a factor of 4. It is now important to identify those aspects of the monolayer structure that are responsible for its behavior under stress. Here we report results from partially disordered ODT layers, and monolayers formed by the shorter molecule octanethiol (OT). A comparison of these chemically similar layers allows us to assess the role of lateral forces and structural defects in maintaining intermolecular order under stress.

## Methods

A detailed description of the mechanical, optical, and chemical design has been published elsewhere.<sup>10</sup> The following summary highlights subsequent changes to the experiment.

The cell consists of a spherical bronze surface that is pneumatically loaded against a flat sapphire prism, producing a small, circular area of high-pressure contact (Figure 1). The observed relationship between applied force, elastic constants, and contact diameter obeys the Hertzian model, allowing computation of the stress normal to the interface.<sup>10,11</sup> In the present experiment, this ranges from 0 (at the circumference) to a maximum between 330 and 660 MPa at the center. Before a contact spot is used for experiments, it is “run in” with several compressions to 1 GPa. Electron microscopy confirms that this procedure plastically smoothes the contact area on the metal. The prism, being smoother to begin with and 20 times harder, is unaffected.

Adsorbed monolayers are introduced to the contact by chemical self-assembly on the bronze substrates. These are approximately cubic, 5 mm along each edge, and cut by spark erosion from the surface of a phosphor bronze ball bearing 50 mm in diameter. After being polished and cleaned, the spherical surface is first evaporatively coated with a

layer of gold  $\sim 200$  nm thick, then prestressed in the contact cell, and then exposed to solutions of alkanethiols in methanol. The resulting monolayers have been thoroughly characterized in the literature.<sup>12</sup> Although the quality of the layers produced by this protocol is somewhat variable, sum-frequency spectra contain internal evidence by which the degree of order can be assessed. Because the defective layers yield interesting results under pressure, disorder was also introduced intentionally. High-quality ODT/Au samples were immersed in an ultrasonically agitated bath of boiling methanol (65 °C) for 90 s, and then rinsed with room-temperature methanol and blown dry. As discussed below, this procedure temporarily disrupts the structure of the monolayer.

Figure 1 shows a schematic cross-section and photograph of the contact. The infrared beam is incident on the contact at  $56^\circ$  and is focused with a spherical  $\text{CaF}_2$  lens. The visible beam approaches at a  $7^\circ$  greater angle of incidence. Foreshortening of the round contact area is compensated by anamorphic focusing of the visible beam by means of two cylindrical lenses ( $f = 175$  mm and  $f = 350$  mm). This yields an approximately circular spot 50  $\mu\text{m}$  in diameter, which defines the area probed in the experiment. This spot is centered by observing scatter from the edges of the contact. The larger infrared spot is then positioned by maximizing the intensity of nonresonant SFG from the gold surface. All beams enter and emerge from the cell p-polarized (ppp).

The visible and infrared laser light is derived from a mode-locked, cavity-dumped Nd:YAG laser (30 ps pulse duration) operating at 20 Hz. Green light at 532 nm ( $18\,797\text{ cm}^{-1}$ ) and mid-infrared light tunable in the 3  $\mu\text{m}$  region ( $2700\text{--}3300\text{ cm}^{-1}$ ) are generated by nonlinear conversion in suitable crystals. Light emerging from the contact is filtered spatially with iris diaphragms, spectrally with a notch filter and monochromator, and temporally by gated detection. At each infrared frequency, the sum-frequency emission is collected on an intensified photodiode array for approximately 1 min. A series of such points is obtained under computer control, normalized by the corresponding values of infrared power, and plotted as a function of infrared frequency.

The resonant SFG band shape is complicated by interference with the nonresonant signal from gold. To determine the center frequency and bandwidth of the underlying Lorentzian resonances, the spectra have been fit to a compound line shape.<sup>7,10</sup> This appears in the figures as a smooth solid curve. Because the absolute nonresonant phase is approximately  $-\pi/2$  in the present experiment, resonances appear as pure dips in the nonresonant background; thus, their frequency, width, and intensity can be assessed qualitatively. The detailed fitting parameters for each of the spectra are available as Supporting Information.

## Results and Discussion

The nonresonant SFG detected from gold in contact with sapphire was 3–4 times more intense than that from gold in air. This is not apparent in the normalized spectra described below. The nonresonant intensity was not further affected by pressure changes.

**The Influence of Chain Length.** Thiols with an even number of carbon atoms between  $\text{C}_6$  and  $\text{C}_{30}$  are known to form structurally similar monolayers.<sup>12</sup> The lower panel of Figure 2 is a schematic cross-section of the layer formed by octadecanethiol ( $\text{C}_{18}$ ) on gold (ODT/Au), showing the van der Waals radii of nearest-neighbor ODT molecules.<sup>13</sup> The illustration is approximate insofar as the out-of-plane twist and tilt of the carbon–carbon backbone is not represented; at room temperature, the methyl rotors are free, and environmental heterogeneity along this coordinate is motionally narrowed.<sup>14</sup>

(11) Johnson, K. L. *Contact Mechanics*; Cambridge University Press: New York, 1985.

(12) Laibinis, P. E.; Whitesides, G. M.; Allara, D. L.; Tao, Y.-T.; Parikh, A. N.; Nuzzo, R. G. *J. Am. Chem. Soc.* **1991**, *113*, 7152–7167.

(13) Pauling, L. *The Nature of the Chemical Bond*, 3rd ed.; Cornell University Press: Ithaca, NY, 1960.

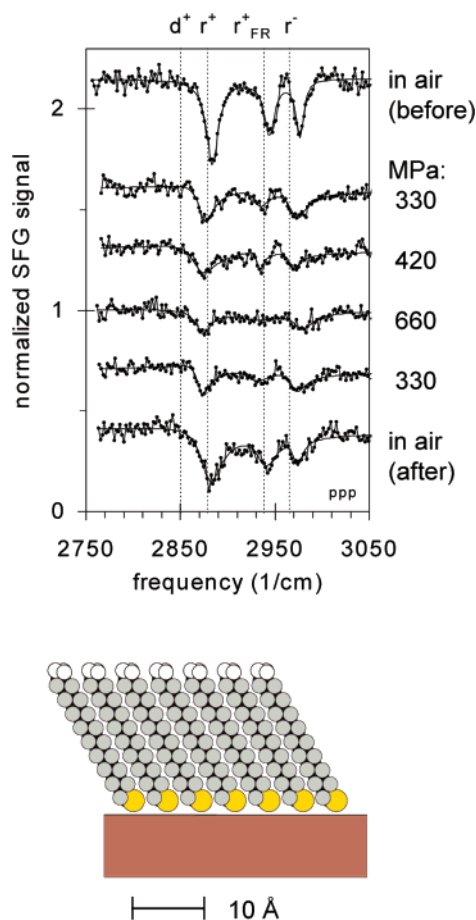


**Figure 2.** Schematic structure of a well-ordered octadecanethiol ( $C_{18}$ ) monolayer on gold, showing the van der Waals contours of sulfur (yellow), methylene hydrogen (gray), and methyl hydrogen (white). Above is a series of normalized sum-frequency spectra obtained during a contact pressure cycle, proceeding from the top down as labeled. Vertical dashed lines indicate typical center frequencies of relevant methyl (r) and methylene (d) C–H stretching vibrations.

The upper panel of Figure 2 is a sequence of sum-frequency spectra showing the effect of a contact pressure cycle on the ODT monolayer. In air, three resonances are observed. These interfere destructively with the frequency-independent background SFG from gold. The resonances are characteristic of the terminal methyl group of ODT. Their standard center frequencies have been marked as dashed vertical lines on the spectra: the symmetric stretch ( $r^+$ ,  $2878\text{ cm}^{-1}$ ), the asymmetric stretch ( $r^-$ ,  $2966\text{ cm}^{-1}$ ), and a Fermi resonance between stretching and bending modes ( $r^+_{FR}$ ,  $2939\text{ cm}^{-1}$ ).<sup>7</sup> In our samples, the initial positions of these resonances are blue-shifted by a few wavenumbers. A fourth dashed line marks the position to the symmetric methylene stretch ( $d^+$ ,  $2850\text{ cm}^{-1}$ ), which is absent from all of the spectra in Figure 2. The fits, using only three resonances, often deviate from the spectra near  $2955\text{ cm}^{-1}$ . This has been attributed by Bain et al. to the out-of-plane asymmetric methyl stretching mode.<sup>15</sup> As this resonance is near the noise level of the present experiment (a consequence of the small laser focus), we have chosen not to include it in the fits.

Proceeding down the figure is a sequence of spectra from a single pressure cycle. They are labeled according to the Hertzian

(14) MacPhail, R. A.; Snyder, R. G.; Strauss, H. L. *J. Chem. Phys.* **1982**, *77*, 1118–1137.

(15) Bain, C. D.; Davies, P. B.; Ong, T. H.; Ward, R. N.; Brown, M. A. *Langmuir* **1991**, *7*, 1563–1566.

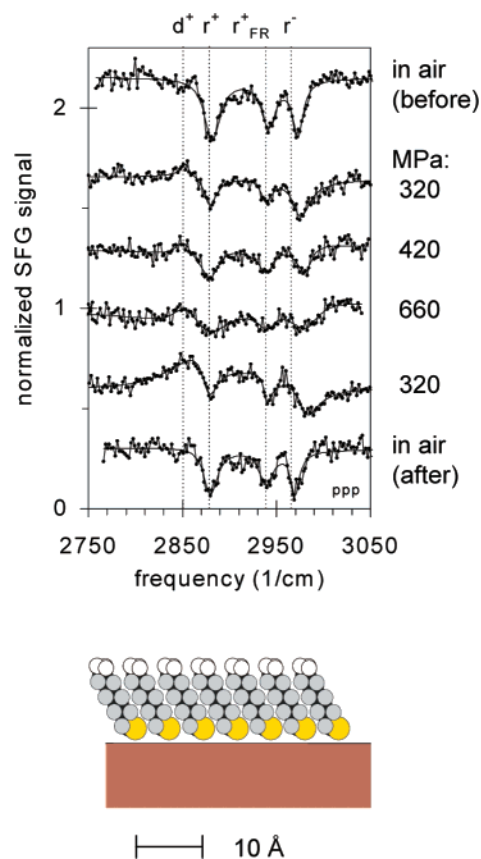


**Figure 3.** Schematic cross-section of a well-ordered octanethiol ( $C_8$ ) monolayer on gold, showing the van der Waals contours of sulfur (yellow), methylene hydrogen (gray), and methyl hydrogen (white). Above is a series of normalized sum-frequency spectra obtained during a contact pressure cycle, proceeding from the top down as labeled. Vertical dashed lines indicate typical center frequencies of relevant methyl (r) and methylene (d) C–H stretching vibrations.

pressure calculated for the center of the contact; averaging within the laser footprint causes less than 10% error.<sup>10</sup> With increasing contact pressure, the ODT/Au peaks in Figure 2 shift to lower frequency, become weaker, and broaden asymmetrically. The Fermi resonance is particularly sensitive. These changes are partially reversed when the pressure is released.

The mechanical behavior of monolayer-coated surfaces is known to depend on chain length.<sup>2,16</sup> Therefore, we chose to compare the  $C_{18}$  thiol (ODT) to the  $C_8$  analogue, octanethiol (OT). The structure of an OT/Au monolayer, illustrated schematically in Figure 3, is similar to that of ODT/Au. Yet the energetics driving its self-assembly are different.<sup>17,18</sup> The lateral binding energy of alkanethiol layers has been estimated as  $1\text{ kcal mol}^{-1}$  per  $\text{CH}_2$  unit, while the surface bond energy is  $\sim 28\text{ kcal mol}^{-1}$ .<sup>19</sup> Layers formed from longer chains (greater than  $C_{12}$ ) are dominated by lateral interchain forces, at the cost of a strained gold surface. Chains shorter than  $C_{12}$  optimize their S-to-Au bonding; nevertheless, steric constraints force the hydrocarbon tails to pack in a similar structure. Consequently,

(16) Liu, Y.; Evans, D. F.; Song, Q.; Grainger, D. W. *Langmuir* **1996**, *12*, 1235–1244.

(17) Fenter, P.; Eisenberger, P.; Liang, K. S. *Phys. Rev. Lett.* **1993**, *70*, 2447–2450.

(18) Ulman, A. *An Introduction to Organic Thin Films: from Langmuir–Blodgett to Self-Assembly*; Academic Press: New York, 1991.

(19) Nuzzo, R. G.; Dubois, L. H.; Allara, D. L. *J. Am. Chem. Soc.* **1990**, *112*, 558–569.



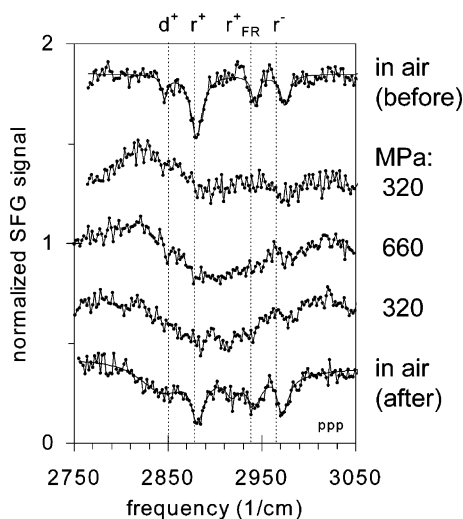


**Figure 4.** Sum-frequency spectra obtained from a defective octadecanethiol ( $C_{18}$ ) layer. The contact pressure cycle proceeds from the top down as labeled. Vertical dashed lines indicate typical center frequencies of relevant methyl ( $r$ ) and methylene ( $d$ ) C–H stretching vibrations.

the SFG spectra of ODT/Au and OT/Au in air are similar, as seen in Figures 2 and 3.

When the shorter-chain monolayer is subjected to a contact pressure cycle, the sequence of SFG spectra (Figure 3) is also similar to that of ODT/Au. The resonances weaken, and the broadening is asymmetric at the intermediate pressure of 320 MPa. This asymmetry is more pronounced than that in the case of ODT/Au, but the pressure-dependent shift is absent.

It has been predicted by computer simulation<sup>20</sup> and observed by AFM<sup>21</sup> that alkanethiol layers on gold remain in place up to at least 800 MPa. Other authors have argued on spectroscopic grounds that adsorbed molecules are not ejected from contacts;<sup>8–10</sup> in the present case, this is certainly true to the extent that the spectra recover with decreasing pressure. The Raman and infrared cross-sections of methyl stretching modes change by only a few percent in our experimental pressure range,<sup>22</sup> so a substantial effect on the molecular SFG cross-section is not expected. Therefore, the reversible weakening observed under pressure indicates that the terminal methyl groups lose their collective orientational bias. This requires either conversion to a centrosymmetric crystalline phase or loss of intermolecular order. Yet the pressure-dependent loss of signal from ODT/Au and OT/Au in contact is unlike disordering phenomena usually observed by SFG spectroscopy, in that the loss of methyl resonances is not accompanied by the appearance of vibrations characteristic of methylene groups ( $d^+$ , 2850  $cm^{-1}$  and  $d^{+FR}$ , 2930  $cm^{-1}$ ).<sup>23</sup> Their nonappearance indicates that the alkane chains remain straight. We conclude that the spectral changes in both ODT and OT are due to rearrangement of the terminal methyl groups, and hence that lateral interactions between hydrocarbon chains (ranging from 7 kcal mol<sup>-1</sup> in the OT layer to 17 kcal mol<sup>-1</sup> in ODT) have no great effect on this process.

**The Influence of Defects.** There is one class of monolayers that behaves differently in contact: those that are poorly ordered before compression. Figure 4 shows the effect of a pressure

cycle on such an ODT/Au layer. The spectrum in air is characteristic of the defective monolayers occasionally produced by the adsorption protocol. The methyl resonances are weaker than those in a well-ordered layer. In addition, a resonance due to the symmetric stretch of methylene groups is resolved ( $d^+$ , 2850  $cm^{-1}$ ). This band is diagnostic of gauche defects in the carbon backbone of the adsorbed layer, from which it follows that the monolayer is not close-packed. In contrast to the defects introduced intentionally (below), the disorder in such samples is permanent. Because prestressing the substrates ensures that their microscopic morphology is consistent from sample to sample, the source of these defects is likely to be chemical contamination. The uncontrolled nature of such samples prohibits us from describing their structure in greater detail. Nevertheless, their behavior under pressure is instructive.

Figure 4 shows the effect of contact pressure on defective monolayer. Already at 320 MPa the methyl group resonances have all but vanished. A broad modulation of the background signal is present, but this cannot be fit or assigned to specific resonances. We note only that its width ( $\sim 100$   $cm^{-1}$ ) is typical of C–H resonances in liquid hydrocarbons. This diffuse feature changes shape during the pressure cycle. The methyl spectrum reappears when the prism is removed; additional, broad features centered at the  $CH_2$   $d^+$  and  $d^-$  resonances have been used to fit the postcontact spectrum in air.

The self-assembly of an alkanethiol layer from solution proceeds in two steps: chemical bonding of a disordered layer to the surface, followed by a period of inter- and intramolecular rearrangement that yields a two-dimensional polycrystal.<sup>24</sup> At room temperature, the equilibrium population of conformational defects is a few percent.<sup>19,20</sup> More defective layers can be produced by interrupting the second step, by mixing two adsorbates, or by disrupting a previously well-ordered monolayer. We have used the latter route to introduce defects in a reproducible way. The normal boiling point of methanol (65 °C) corresponds to the temperature of a first-order melting transition in the ODT/Au system.<sup>17</sup> When an ordered  $C_{18}$  monolayer is immersed in boiling methanol for 90 s, its sum-frequency spectrum changes from the type shown in Figure 5a to that in Figure 5b. Bands  $r^+$  and  $r^{+FR}$  develop strong low-frequency shoulders where methylene modes are expected:  $d^+$  (the symmetric stretch) at 2850  $cm^{-1}$ , and  $d^{+FR}$  (its Fermi resonance with a bending mode) at 2930  $cm^{-1}$ . As shown,  $d^+$  can appear as a resolved peak. Because methanol contains no methylene groups, we assign the signals to disordered alkane chains in the monolayer itself. These features are temporary; the well-annealed, purely methyl monolayer spectrum recovers over a period of days.

During initial self-assembly of these layers, intermolecular order progresses from the thiol headgroups outward to the methyl tail, and finally to the consolidation of rotational domains.<sup>24</sup> Therefore, melting and solvation are expected to begin at domain boundaries and proceed from the methyl tails inward. Indeed, there is evidence that contact with solvents modifies methylene groups near the outer surface of the monolayer.<sup>25</sup> Therefore, the defects produced by boiling solvent will be gauche conformers near the outer surface of the

(20) Siepmann, J. I.; McDonald, I. R. *Phys. Rev. Lett.* **1993**, *70*, 453–456.

(21) Liu, G.-y.; Salmeron, M. B. *Langmuir* **1994**, *10*, 367–370.

(22) Ferraro, J. R. *Vibrational Spectroscopy at High External Pressure: The Diamond Anvil Cell*; Academic Press: New York, 1984.

(23) Miranda, P. B.; Pflumio, V.; Saijo, H.; Shen, Y. R. *Thin Solid Films* **1998**, *327*, 161–165.

(24) Himmelhaus, M.; Eisert, F.; Buck, M.; Grunze, M. *J. Phys. Chem. B* **2000**, *104*, 576–584.

(25) Ong, T. H.; Davies, P. B.; Bain, C. D. *Langmuir* **1993**, *9*, 1836–1845.

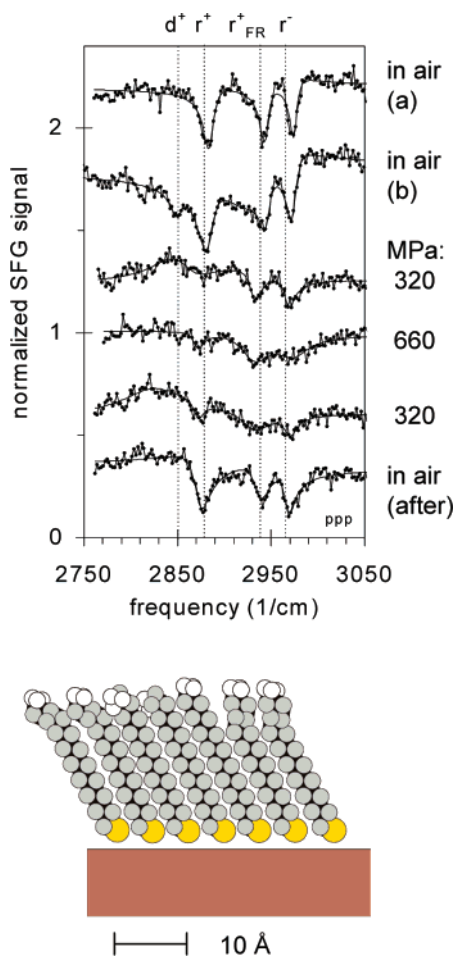


**Figure 5.** Schematic structure of an octadecanethiol ( $C_{18}$ ) monolayer that has been disrupted by melting. Above is a series of normalized sum-frequency spectra obtained before heat treatment (a), after heat treatment (b), and during a contact pressure cycle, proceeding from the top down as labeled. Vertical dashed lines indicate typical center frequencies of relevant methyl (r) and methylene (d) C–H stretching vibrations.

monolayer, perhaps stabilized by methanol. The volume of defects and inclusions must be accommodated by desorption or a decreased overall tilt. Such a structure is illustrated schematically in the lower panel of Figure 5.

The behavior of this disrupted layer under pressure is intermediate between that of well-annealed layers and permanently defective ones. Although methyl resonances are still resolved at 320 MPa, there is a broad modulation of the nonresonant background. At 660 MPa, the resonances are washed out further, and their return with decreasing pressure is incomplete. Nevertheless, when the prism is removed, the contact spot yields a well-resolved methyl spectrum.

Whenever methyl bands are observed under pressure, the features have a conspicuous asymmetry at the intermediate pressure of 320 MPa: the bands no longer fit a single resonance in pure destructive interference with the background. Where the asymmetry is small, as in ODT, the band shapes can be fit by shifting the phase of the nonresonant background. However, this interpretation of the asymmetry is problematic. The phase of SFG signals depends on the electronic structure of the interface, the Fresnel factors that govern its classical optical behavior, and the average tilt of the transition dipoles involved. Neither the susceptibility of gold nor the classical optics of the interface change with changing pressure, because the observed

nonresonant signal level is constant. Also a change of molecular orientation is not sufficient to account for the large asymmetry that appears in the spectra of OT (Figure 3) and disrupted ODT (Figure 5) at 320 MPa. In these cases, because there is a substantial positive-going signal at low frequency, a shifted nonresonant phase does not yield accurate fits to the data. An additional, diffuse resonance, of opposite sign to the methyl modes, has to be included. It is centered near  $2860\text{ cm}^{-1}$  and is  $80\text{--}100\text{ cm}^{-1}$  wide.

Similar components have been reported previously in the SFG literature. In a detailed study of the formation of docosanethiol ( $C_{22}$ ) layers on gold, Himmelhaus and co-workers observed a broad ( $25\text{--}40\text{ cm}^{-1}$ ) low-frequency resonance ( $2813\text{ cm}^{-1}$ ), of opposite sign to methyl and methylene features, during the earliest stages of adsorption.<sup>24</sup> This “soft mode” is attributed to alkyl chains that are in contact with the gold, hence electronically perturbed, when low coverage permits. It is conceivable that contact pressure could force alkane chains to interact with the gold substrate, but unlikely that this effect would be reversed at the highest pressures. In the same study, a sharp signal of opposite phase at  $2860\text{ cm}^{-1}$  was assigned to the outermost methylene groups during annealing. Weak resonances of opposite sign have also been reported by Duffy et al., in a study of Langmuir–Blodgett films on iron.<sup>26</sup> In this case, positive-going methylene signals were assigned to a second, inverted layer adsorbed atop the first. Defects of this type may be expected to disappear with increasing pressure, when free volume is energetically costly. In the present case, a similar feature is affecting all of the in-contact spectra at 320 MPa. It is a minimal indication that the methylene groups along the hydrocarbon chains have been forced into a heterogeneous distribution of noncentrosymmetric conformations.

**Comparison with Mechanical Measurements.** Much of the nanotribological literature is concerned with the observation of chemically specific forces between surfaces, so the mechanical loads applied are comparable to adhesive interactions. Stresses in the present experiment are 2–3 orders of magnitude greater. Some direct measurements of nanomechanical behavior under these conditions have been published, and these lead to a qualitative picture in accord with the spectroscopy. During high-load nanotribological experiments, it is observed that alkane-thiolate layers persist despite plastic indentation of the gold substrate and recover from severe flattening on a time scale of seconds.<sup>27</sup> Furthermore, although disruption of the structure of such layers has been observed by frictional force microscopy, the critical load at which this occurs is independent of chain length.<sup>21</sup> With decreasing surface density, adsorbed monolayers become more compressible<sup>28</sup> and exhibit larger frictional forces.<sup>29</sup> Discrete pressure-induced interchain rearrangement events have been observed in monolayers chemisorbed to mica, but only at submonolayer (island) coverage.<sup>30</sup> These results confirm the importance of defects and free volume in allowing rearrangement under mechanical stress.

(26) Duffy, D. C.; Friedmann, A.; Boggis, S. A.; Klenerman, D. *Langmuir* **1998**, *14*, 6518–6527.

(27) Thomas, R. C.; Houston, J. E.; Michalske, T. A.; Crooks, R. M. *Science* **1993**, *259*, 1883–1885.

(28) Chen, Y. L.; Helm, C. A.; Israelachvili, J. N. *Langmuir* **1991**, *7*, 2694–2699.

(29) Lee, S.; Shon, Y.-S.; Colorado, R., Jr.; Guenard, R. L.; Lee, T. R.; Perry, S. S. *Langmuir* **2000**, *16*, 2220–2224.

(30) Barrena, E.; Kopta, S.; Ogletree, D. F.; Charych, D. H.; Salmeron, M. *Phys. Rev. Lett.* **1999**, *82*, 2880–2883.

The most detailed microscopic view of structural changes is provided by computational models. Mikulski and Harrison performed molecular dynamics simulations of C<sub>18</sub> chains grafted onto diamond, with pressure and shear applied by a hydrogen-terminated diamond counterface.<sup>4</sup> Whereas saturated monolayers retained their crystalline order to 33 GPa, the densification of loosely packed layers (30% vacant) occurred as soon as “appreciable pressure” was applied, with a conspicuously disordered result. The diffuse, liquidlike SFG spectrum of compressed defective monolayers in contact is in full agreement.

Simulation and experiment both find that the conformational changes in a densely packed layer are less drastic. In another simulation of hydrocarbon-terminated diamond, contact and shear created gauche defects near the ends of the chains.<sup>5</sup> A system chemically analogous to the present experimental samples was modeled by Siepmann and McDonald.<sup>20</sup> In their Monte Carlo simulation of hexadecanethiol/Au under contact pressure, a stress of ~6 GPa increased the molecular tilt by 20° and raised the population of terminal gauche defects from 6 to 38%. These effects were approximately linear with applied pressure, so their magnitude under the conditions of the present experiment is expected to be an order of magnitude lower. In the following section, the sensitivity of resonant SFG signal to these types of changes is quantified.

**Sensitivity to Orientational Changes.** The pump lasers drive a macroscopic polarization within the sample that radiates light at the sum frequency. Because the resonant nonlinear susceptibility is a combination of individual molecular contributions, it is sensitive to the distribution of molecular orientations. For the methyl groups in question here, two of the relevant degrees of freedom (rotation about the C<sub>3</sub> axis, and its projection onto the surface) are evenly distributed. Therefore, the changes observed as a function of pressure reflect a redistribution of tilt angles. This sensitivity to tilt can be quantified by formalizing some of the optical and statistical constraints. The equations have been developed by Hirose<sup>31</sup> and applied to the interpretation of SFG spectra by Hirose et al.,<sup>32</sup> Bell et al.,<sup>33</sup> and Duffy et al.<sup>26</sup>

The sum-frequency, visible, and infrared electric field intensities  $I_{\text{SFG}}$ ,  $I_{\text{VIS}}$ , and  $I_{\text{MIR}}$  are related to the macroscopic second-order susceptibility  $\chi$  as follows:

$$I_{\text{SFG}} \propto I_{\text{VIS}} I_{\text{MIR}} |L_{\text{SFG}} K_{\text{VIS}} K_{\text{MIR}} \chi|^2 \quad (1)$$

Each  $K$  is a constant of proportionality between the incident propagating field and the local field at the interface. Similarly,  $L$  is the fraction of SFG polarization that radiates toward the detector. In the following, we include only macroscopic optical effects in  $L$  and  $K$ , as described by Fresnel amplitude coefficients. Resolved into Cartesian coordinates, the susceptibility is a third-rank tensor  $\chi_{jkl}$  with each component indexed according to the directions of the sum-frequency, visible, and infrared fields. The effective susceptibility is a superposition of these components from the metal  $\chi_{jkl}^{\text{NR}}$  (which have been measured for polycrystalline Au/hexadecanethiol<sup>34</sup>) and resonant compo-

nents  $\chi_{jkl}^{\text{R}}$ . The latter result from the hyperpolarizability  $\beta$  of individual molecules:  $\chi_{jkl}^{\text{R}} \propto \langle \beta_{jkl} \rangle$ , where  $\langle \rangle$  represents orientational averaging appropriate to the sample. With these developments, eq 1 becomes

$$I_{\text{SFG}} \propto I_{\text{VIS}} I_{\text{MIR}} \left| \sum_{j,k,l} L_j K_{\text{VIS},k}^{\text{T}} K_{\text{MIR},l}^{\text{T}} \chi_{jkl}^{\text{NR}} + a \sum_{j,k,l} L_j K_{\text{VIS},k}^{\text{R}} K_{\text{MIR},l}^{\text{R}} \langle \beta_{jkl} \rangle \right|^2 \quad (2)$$

By defining the  $z$  axis normal to the surface, only 4 of the 27  $\chi_{jkl}$  are not exactly zero:  $\chi_{xxz}$ ,  $\chi_{xzx}$ ,  $\chi_{xxz}$ , and  $\chi_{zzz}$ . In the present experiment, all electric fields are polarized in the plane of incidence (ppp); the  $x$  axis is defined in this plane, normal to  $z$ . In eq 2, we recognize that the nonresonant response is driven by fields transmitted into the gold; hence the appropriate Fresnel factors  $K^{\text{T}}$  are different than those for the adsorbate, which is in the incident plus reflected field described by  $K^{\text{R}}$ . Numerical values of the  $L$ ,  $K$ , and other optical parameters are tabulated in the Supporting Information. Because of the high infrared reflectivity of gold,  $K_{\text{MIR},x}^{\text{R}}$  is much smaller than the factor along  $z$ , so all terms containing it have been dropped from the computation. A scaling factor  $a$  adjusts the overall amplitude of the resonant response relative to the nonresonant background; this is necessary if the elements of  $\chi^{\text{NR}}$  and  $\beta$  are obtained from different, arbitrarily scaled sources. Factor  $a$  also absorbs the constant of proportionality between the  $\chi^{\text{R}}$  and  $\beta$ .

When the prism is present, refractive index matching allows greater transmission into the substrate and thereby more intense SFG from gold. Including the external prism faces, eq 2 predicts that the nonresonant signal level will increase by a factor of 2.3 relative to its intensity in air. The greater experimental value of 3–4 indicates other influences: elastic flattening of the surface, perhaps, or modification of the interfacial fields by the birefringence of sapphire. These cannot be responsible for pressure-dependent effects, however. The nonresonant signal level is a sensitive probe of the local fields and morphology, and yet it does not change over the range of contact pressures studied here.

We can now consider the SFG intensity at the center of a well-resolved resonance, such as the symmetric methyl stretch  $r^+$ . This mode is invariant under rotation about the methyl C<sub>3</sub> axis, and azimuthally averaged by multiple rotational domains, with the following result:<sup>31</sup>

$$\langle \beta_{zzz} \rangle = \frac{1}{4} [\langle \cos \theta \rangle (3\beta_{ccc} + \beta_{aac}) - \langle \cos 3\theta \rangle (\beta_{aac} - \beta_{ccc})] \quad (3)$$

$$\langle \beta_{xzx} \rangle = \frac{1}{8} [\langle \cos \theta \rangle (\beta_{ccc} + 7\beta_{aac}) + \langle \cos 3\theta \rangle (\beta_{aac} - \beta_{ccc})] \quad (4)$$

Here  $\theta$  is the only remaining orientational parameter, tilt of the C<sub>3</sub> axis from the surface normal. The following computation is relatively insensitive to  $\beta_{aac}/\beta_{ccc}$ , a representative value of which can be obtained from the literature ( $\beta_{aac}/\beta_{ccc} = 3.4$ ).<sup>33</sup> In air, the peak of  $r^+$  dips to 0.58 of the nonresonant background; this value of  $I_{\text{SFG}}$  is used to determine  $a$ . Equations 2–4 can then describe the dependence of the SFG signal on the pure tilt angle with the prism in place. The result is plotted in Figure 6, which has been normalized to the nonresonant background intensity. Even without a modified tilt angle ( $\theta \approx 0$ ), the peak is reduced to 0.85. With increasing tilt, the depth of the resonance is

(31) Hirose, C.; Akamatsu, N.; Domen, K. *Appl. Spectrosc.* **1992**, *46*, 1051–1072.

(32) Hirose, C.; Yamamoto, H.; Akamatsu, N.; Domen, K. *J. Phys. Chem.* **1993**, *97*, 10064–10069.

(33) Bell, G. R.; Bain, C. D.; Ward, R. N. *J. Chem. Soc., Faraday Trans.* **1996**, *92*, 515–523.

(34) Buck, M.; Eisert, F.; Grunze, M.; Träger, F. *Appl. Phys. A* **1995**, *60*, 1–12.



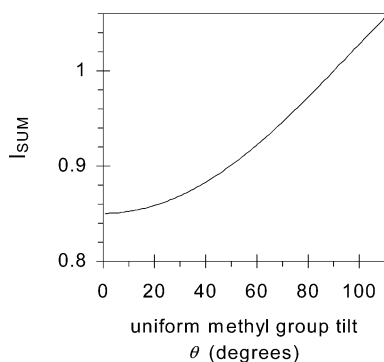


**Figure 6.** Dependence of the sum-frequency signal (at the center of  $r^+$ ) on the uniform tilt  $\theta$  of the methyl groups, from eqs 2–4.

expected to decrease until  $\theta = 90^\circ$ , when all orientational anisotropy is washed out by azimuthal averaging. Greater tilts yield a resonant polarization of opposite sign; hence  $I_{\text{SFG}} > 1$ .

In the well-formed ODT/Au layer, the intensity of  $r^+$  falls from 0.58 in air to 0.86 at 320 MPa and to 0.90 at 660 MPa (similar values describe OT/Au). This result may be compared to Figure 6, under the assumption that tilt is the only term in eqs 2–4 that depends on pressure. The initial loss of signal is evidently an optical consequence of the sapphire counterface, as it requires no modification of the tilt. A subsequent uniform tilt of  $50^\circ$  would reduce the signal to the observed high-pressure value. If this were to be achieved by tilting the entire molecule, it is far beyond the magnitude predicted by simulation ( $\sim 2^\circ$ ) or observed under AFM tips. Furthermore, as the linear compressibility of molecular crystals is only a few percent per GPa,<sup>21</sup> the required loss of specific volume is not plausible. Therefore, the methyl groups must reorient by a mechanism other than whole-chain tilt.

In the computer simulations discussed above, the orientation of methyl groups was altered mainly by conformational changes near the outer surface of the monolayers. Even with the force applied by a supernaturally flat counterface, terminal gauche defects in particular appeared. These defects are local minima in the conformational potential, reached by  $120^\circ$  rotation about the penultimate C–C bond. If the methyl  $C_3$  axis is initially normal to the surface, then in gauche conformers it is tilted by the tetrahedral angle. A range of tilt angles can be introduced to the formalism by performing the final orientational average in eqs 3 and 4. To model the effect of gauche defects, the bracketed expressions are convoluted by a discrete distribution of tilt angles

$$g(\theta) = (p/2)\delta(\theta - 109^\circ) + (p/2)(\delta + 109^\circ) + (1 - p)\delta(\theta) \quad (5)$$

where  $\delta$  is the Dirac delta function, and  $p$  is the fraction of terminal gauche defects. The result is plotted in Figure 7, normalized again to the nonresonant background. The depth of the resonant signal is expected to decrease with the increasing fraction of defects, until ultimately a positive-going peak appears. At  $p = 1$ , it necessarily reaches the same value as a uniform tilt of  $109^\circ$ . It is a simplification to assume that the undisturbed methyl  $C_3$  axes are exactly normal to the surface. The orientation of this group has been difficult to measure, but for the series of thiols with an even number of carbon atoms (including ODT and OT), a substantially normal orientation has been deduced.<sup>12,19</sup>

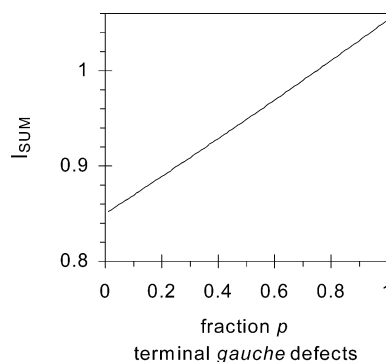


**Figure 7.** Dependence of the sum-frequency signal (at the center of  $r^+$ ) on the fraction  $p$  of methyl groups in gauche conformations, from eqs 2–5.

Figure 7 shows that a fraction  $p = 0.25$  decreases the resonant signal to 0.90 of background, as observed at 660 MPa. The relative freedom of the terminal methyl units to adopt this conformation has been observed during annealing<sup>24</sup> and under solvents,<sup>25</sup> but not to this extent. The Monte Carlo prediction  $p \approx 0.03$  is also considerably lower. A greater fraction is to be expected in the contact experiment, because the real solid counterface presents stiff chemical irregularities that can force the methyl groups aside.<sup>5</sup> At least the defect population required under this interpretation of the spectra does not violate any fundamental packing constraints.

The present SFG measurement is not sufficiently sensitive to support a detailed orientational analysis through angle- or polarization-dependent studies. The model in Figures 6 and 7 shows simply that a redistribution of methyl group orientations could attenuate resonant SFG signals to the extent observed under contact pressure, while a redistribution of whole-molecule tilts would have to be unreasonably large. Two further observations are consistent with an increased population of gauche defects. The first is a shift in the relative intensity of the in-phase ( $r^+$ ) and out-of-phase ( $r^-$ ) modes of the methyl group, in keeping with the different orientations of their transition dipoles. At 660 MPa,  $r^-$  is consistently more intense relative to  $r^+$  than it is in air. Second, an additional, diffuse spectroscopic component is evident at intermediate pressures. Both its position and its negative sign are suggestive of methylene groups in a strongly perturbed, heterogeneous environment.

## Conclusion

We have compared the behavior of four closely related monolayers during compression, using the persistence of methyl C–H stretching modes as an indicator of orientational order within the layer. The sensitivity of long- and short-chain layers is similar; therefore, the absence of lateral stabilization within the layer alone does not make it susceptible to disruption. On the other hand, the strong intermolecular stabilization of thicker layers does not protect them when they are poorly packed or defective. Such layers disorder more easily than their well-packed analogues and show greater irreversible effects.

Other groups have observed a large decrease of resonant SFG signal level (a factor of 300, after classical optical corrections) from compressed Langmuir–Blodgett films.<sup>8,9</sup> The present results suggest that the less dense packing of these physically formed layers allows them to relax significantly when compressed. The weak and diffuse SFG spectra of defective layers under stress are to be expected from a partially oriented liquid

or glass, but are otherwise uninformative. In these cases, published molecular dynamics simulations of confined alkane layers provide an atomistic picture of the disordering effect of pressure.

It is a peculiarity of alkanethiolated gold that the strong chemisorption drives both long and short molecules to become well-ordered and densely packed. For such monolayers, pressure-dependent changes in the SFG spectra document the structural changes that occur under pressure. The small frequency shifts and heterogeneous broadening are similar to effects observed under solvents. Unlike solvents, however, solid/solid contact strongly attenuates the resonant SFG intensity. Most of the physical parameters that determine SFG intensity are not sensitive to our modest pressure range (as evinced by the nonresonant SFG level, which is unaffected), so we are led to believe that the distribution of molecular orientations changes.

Both the sensitivity of the SFG signal to orientational effects and the molecular degrees of freedom are strongly constrained. By comparing these, we find that an increased population of terminal gauche defects is likely to be the principal conformational change under pressure. Here, again, our observations from the experimental contact are in detailed agreement with computer simulations.

**Acknowledgment.** This work was supported by the Ernest Oppenheimer Memorial Trust.

**Supporting Information Available:** Tables S1–S4 specifying the band shape parameters that yield the best-fit curves in Figures 2–5, and table S5 of the optical parameters used to evaluate eq 2 (PDF). This material is available free of charge via the Internet at <http://pubs.acs.org>.

JA027128W